Semicond. Sci. Technol. 8 (1993) S102–S105. Printed in the UK

Electronic band structure of far-infrared $Ga_{1-x}In_xSb/InAs$ superlattices

R H Miles†, J N Schulman†, D H Chow† and T C McGill‡

† Hughes Research Laboratories, Malibu, CA 90265, USA
‡ California Institute of Technology, Pasadena, CA 91125,USA

Abstract. Results of tight-binding and eight-band $k \cdot p$ calculations of the electronic band structure of long wavelength $Ga_{1-x}In_xSb/InAs$ superlattices are compared with experimental energy gap and absorption coefficient data. The effective masses, band splittings and absorption coefficients observed in this system illustrate the potential of these structures for application in focal plane array systems demanding high detectivities or relaxed cooling requirements. Comparisons with $Hg_{1-x}Cd_xTe$, the industry standard, are particularly favourable at longer wavelengths (8–12 μm and beyond), due to both a substantial reduction in tunnel currents and a suppression of impact ionization noise processes. We also find that the InSb- or $Ga_{1-x}In_xAs$-like nature of the interfaces should affect the energy gap of a $Ga_{1-x}In_xSb/InAs$ superlattice, and that substantially larger optical absorption coefficients are to be expected in structures with InSb-like interfaces. Our calculations are in agreement with experimental absorption spectra and with observed dependences of energy gaps on interfacial chemistry, measured in samples in which the nature of the interfaces was controlled through appropriate shuttering sequences and use of interrupts during growth by molecular beam epitaxy.

1. Introduction

Recent work on $Ga_{1-x}In_xSb/InAs$ superlattices has been motivated by infrared detector applications for these structures [1, 2], particularly in the 8–12 μm atmospheric transmission band. Brought to maturity, detectors based on these superlattices could be expected to achieve background-limited performance at operating temperatures higher than those of HgCdTe-based systems. Such superlattice detectors might also prove to be more readily manufactured and more robust than the II–VIs currently used, owing to compatibility with mainstream III–V processing technology and to the enhanced structural stability of the material, respectively.

While detectors rivaling $Hg_{1-x}Cd_xTe$ have yet to be fabricated from $Ga_{1-x}In_xSb/InAs$ superlattices, considerable strides have been made in their development over the past couple of years. Molecular beam epitaxial growth conditions yielding superlattices that are essentially structurally ideal [3] have been established [4–6]. Background doping levels, previously in the range 10^{16}–10^{17} cm^{-3}, are now routinely in the low 10^{15} cm^{-3} [7], and structures with long wavelength energy gaps now yield appreciable photoluminescence [8]. A number of theoretical predictions have been borne out by experiment, including the dependence of the superlattice energy bandgap on layer thicknesses and compositions (up to $x = 0.30$) [9], the magnitude of the optical absorption coefficient in 8–12 μm superlattices [5, 10] and the approximate values of the electron and hole effective masses [11, 12].

In this paper we address the properties of $Ga_{1-x}In_xSb/InAs$ superlattices with intrinsic photoresponse beyond 12 μm. The considerable magnitude of tunnelling noise currents and the sensitivity of these currents to small variations across a wafer have mitigated against the application of large area $Hg_{1-x}Cd_xTe$ detectors in this spectral region. As a consequence, extrinsic detectors such as those based on doped Si are currently the standard beyond 12 μm, despite the considerable sacrifices in operating temperature or detectivity associated with extrinsic detectors. We predict both a marked reduction in tunnel currents in $Ga_{1-x}In_xSb/InAs$ superlattice detectors with far-infrared cut-offs, and a comparative insensitivity of these currents to variations across an array, relative to $Hg_{1-x}Cd_xTe$. These properties derive from the larger effective masses found in these superlattices, and from qualitative differences between the band structures in the two cases. Lastly, we use a tight-binding model to examine effects of interfacial chemistry on the energy gaps and absorption coefficients of these superlattices. We find that the interfaces have a sizable effect on these properties, particularly at longer wavelengths. Our results are consistent with the limited experimental data on this subject.

2. $k \cdot p$ calculations

Two means were used to calculate the electronic band structure of narrow gap $Ga_{1-x}In_xSb/InAs$ superlattices.

0268-1242/92/01S102+04$07.50

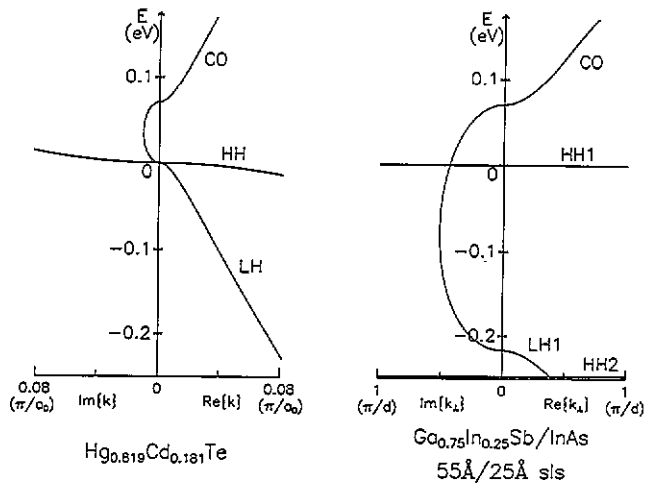

Figure 1. Comparison of $Hg_{1-x}Cd_xTe$ and $Ga_{1-x}In_xSb/InAs$ superlattice electronic band structures, illustrating the considerable magnitude of the imaginary wavevector in the superlattice gap and the shift of the first light-hole state (LH1) more than an energy gap below the heavy hole ground state (HH1). Real wavevectors (Re{k}) are plotted to the right of the energy axes and imaginary wavevectors (Im{k}) to the left. The out-of-plane wavevector ($k_\perp$) is plotted in the case of the superlattice.

An eight-band $k \cdot p$ model was used to determine energy gaps, band splittings and effective masses, neglecting interface effects; and a two-band tight-binding model was applied to estimate the magnitude of effects due to interfaces and the characteristics of the resulting optical absorption spectra. Energy gaps calculated by the two methods are in close agreement when interface effects are neglected in the tight-binding analysis.

The $k \cdot p$ calculation has been described in detail elsewhere [13, 14]. We use a second-order $k \cdot p$ model incorporating spin–orbit splitting and strain. Effects derived from bands outside the basis set (which consists of the two lowest conduction band states and six highest valence band states) are described by Luttinger parameters. Where available, parameters were taken from Lawaetz [15]; the remainder were taken from the Landolt-Börnstein series [16]. Strain is incorporated through a three-parameter deformation potential [17], describing hydrostatic shifts to the energy gap and [100] and [111] uniaxial shifts. We assume an $InAs/Ga_{1-x}In_xSb$ valence band offset of 560 meV [18], regardless of alloy composition, and further assume that hydrostatic strain does not affect this value. Our model yields energy gaps that are in good agreement with those determined from photoconductive thresholds [9], and in-plane effective masses consistent with experimental observations on superlattices with 8–12 μm cut-offs [12].

Figure 1 shows calculated 77 K dispersion curves for a $Hg_{0.819}Cd_{0.181}Te$ alloy and a 25 Å/55 Å $Ga_{0.75}In_{0.25}Sb/InAs$ superlattice. Real wavevectors are plotted to the right of the energy axes, and imaginary wavevectors (corresponding to the reciprocal of the decay length governing tunnelling across a forbidden region) are plotted to the left. Both structures have energy gaps of 70 meV. We calculate electron effective masses of $m_e^* = 0.00534\,m_e$ and $m_{e,\perp}^* = 0.0215\,m_e$, respectively, for the two cases (we find the electron effective mass in the superlattice to be nearly isotropic). As can be seen from the magnitude of the imaginary wavevectors in the energy gaps, both the zone-centre splitting of the heavy- and light-hole bands and the increased electron effective mass should greatly reduce tunnel currents in the superlattice. The splitting of the valence band states is also predicted to suppress Auger recombination in p-type structures by reducing the phase space available for this process [19]. Initial calculations have shown this to be so [20]. While the effective masses are considerably greater in the superlattice than in the alloy, we also find them to be less sensitive to energy gap fluctuations; a 10 meV reduction in energy gap (corresponding to a 0.6% change in $Hg_{1-x}Cd_xTe$ alloy composition, or a 6.8% change in superlattice layer thickness) results in a 14% reduction in m_e^* for the $Hg_{1-x}Cd_xTe$ alloy (to $0.00460\,m_e$), but only a 0.9% reduction (to $0.0213\,m_e$) in the superlattice. These benefits suggest that $Ga_{1-x}In_xSb/InAs$ superlattices are particularly well suited to large area, long wavelength infrared (LWIR) detector applications at wavelengths that have proven inaccessible to $Hg_{1-x}Cd_xTe$ for practical reasons. Furthermore, brought to maturity, such detectors would display higher detectivities and/or higher operating temperatures than $Hg_{1-x}Cd_xTe$ sensors (either would greatly outperform extrinsic detectors in these regards).

3. Effects due to interfaces

Two types of interface are possible in, e.g., a (100) GaSb/InAs superlattice: an 'InSb-like' interface, in which planes of atoms are stacked in the growth direction as follows:

··· Ga Sb Ga **Sb In** As In As In As **In Sb** Ga Sb Ga ···

or a 'GaAs-like' interface:

··· Ga Sb **Ga As** In As In As In As **In As** Ga Sb Ga ···

Control of the interfacial chemistry, achieved through appropriate shuttering sequences and use of interrupts during growth by molecular beam epitaxy, has been demonstrated previously [21, 22].

We employ a two-band tight-binding model to assess the effects of the interfaces on the electronic properties of these quaternary superlattices. The model allows individual layers of In, Ga, As or Sb atoms (or mixtures thereof) to be identified at each atomic plane. In the wide well and barrier limit, the energy bands and wavefunctions are essentially those of two-band envelope function models. Aside from strain effects, the model has been described previously [23]. The input parameters consist of the bulk bandgaps and band discontinuities for the on-site energy parameters of the

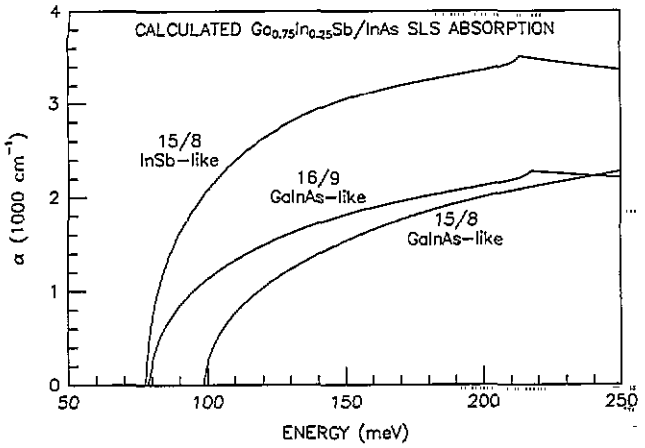

Figure 2. Absorption coefficients calculated for 8 ML/15 ML $Ga_{0.75}In_{0.25}Sb$/InAs superlattices with InSb- and $Ga_{0.75}In_{0.25}As$-like interfaces and a 9 ML/16 ML structure with $Ga_{0.75}In_{0.25}As$-like interfaces. The 9 ML/16 ML case was chosen to preserve both the 15.5 μm energy gap and the mean level of strain in the superlattice.

model, and the bulk effective masses for the transfer matrix elements.

Strain is included through deformation potentials. 'Local' conduction and valence band edges are found for each atomic bilayer, based on the lattice strain and deformation potentials for the local atomic composition. This determines the on-site parameters. The shifted band edges are then used to find the effective mass in the locally strained material using a three-band $\boldsymbol{k}\cdot\boldsymbol{p}$ formula [24]. The tight-binding transfer matrix elements are then determined from the local effective masses.

An interface atom is treated as having the average of properties of the bulk semiconductor formed by pairing with the atom to its right and those formed by pairing to its left. For example, the on-site interface As parameters at an In–As–Ga–Sb interface were taken to be averages of InAs and GaAs on-site As parameters. Similarly, the Ga parameters were set to be averages of GaAs and GaSb parameters.

Figure 2 shows optical absorption curves derived from our tight-binding model. Three cases are presented: 8 ML/15 ML† $Ga_{0.75}In_{0.25}Sb$/InAs superlattices with (1) InSb-like interfaces and (2) $Ga_{0.75}In_{0.25}As$-like interfaces, and (3) a 9 ML/16 ML $Ga_{0.75}In_{0.25}Sb$/InAs superlattice with $Ga_{0.75}In_{0.25}As$-like interfaces (chosen to have approximately the same energy gap and strain level as (1)). The figure illustrates both the shift in energy gap upon changing the interfacial chemistry, and the desirability of InSb-like interfaces for achieving large LWIR absorption coefficients with abrupt thresholds. The magnitude of the energy gap shift is in fair agreement with experiment. A previous study [22] found a shift of 25 meV for a 8 ML/13 ML $Ga_{0.75}In_{0.25}Sb$/InAs superlattice. While this is somewhat larger than the 15 meV we calculate for this case, we note that small changes in layer thicknesses will significantly alter the

† We adopt the (arbitrary) convention of labelling superlattices by indicating the number of group-III monolayers in each layer of the superlattice.

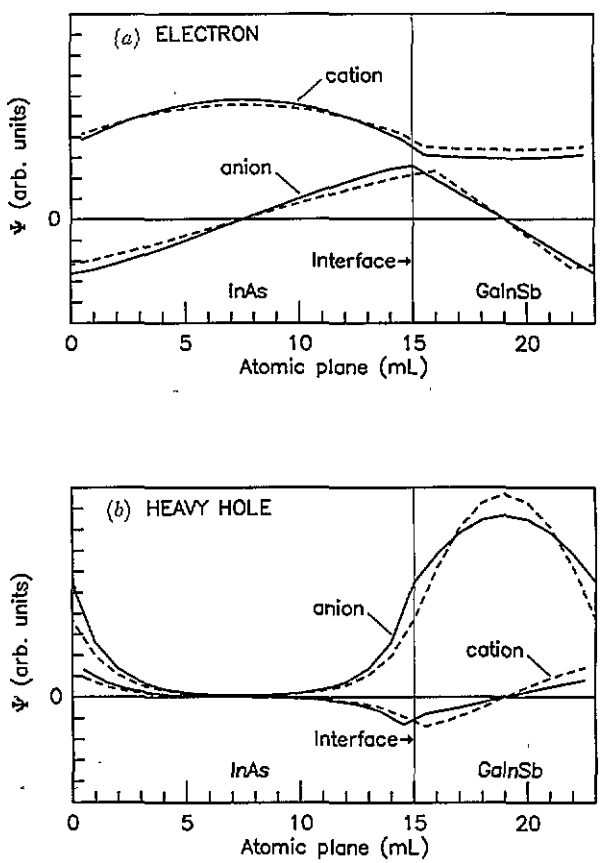

Figure 3. Zone-centre (*a*) electron and (*b*) hole tight-binding wavefunctions for 8 ML/15 ML $Ga_{0.75}In_{0.25}Sb$/InAs superlattices with InSb-like (full curves) and $Ga_{0.75}In_{0.25}As$-like (broken curves) interfaces. Both cation and anion wavefunctions are plotted.

magnitude of this dependence (as illustrated by the shift of more than 20 meV for the case chosen for figure 2). Our calculations are in excellent agreement with previously published absorption coefficient data [10], assuming InSb-like interfaces. We are not aware of experimental absorption data for samples with $Ga_{1-x}In_xAs$-like interfaces.

Tight-binding wavefunctions for zone-centre states are presented in figure 3. Electron (*a*) and hole (*b*) wavefunctions are shown for the 8 ML/15 ML InSb-like and $Ga_{0.75}In_{0.25}Sb$-like cases for which absorption coefficients were given in figure 2. The increased valence-to-conduction band oscillator strength calculated for the former arises from two factors: wavefunction overlap at the interfaces increases on switching from a highly strained monolayer of $Ga_{0.75}In_{0.25}As$ to one of InSb in this region; and the requirement of achieving the same energy gap necessitates wider layers in the $Ga_{0.75}In_{0.25}As$ case, further isolating the electrons and holes in the InAs and $Ga_{0.75}In_{0.25}Sb$ layers, respectively.

Our calculations neglect the possibility of a dependence of the band offsets on interface strain. Such an effect has been predicted in the $InAs/Al_{0.8}Ga_{0.2}As_{0.14}Sb_{0.86}$ superlattice system [25]. A calculation in which a strain-dependent band offset was assumed has yielded a theoretical energy gap in agreement with photoluminescence data from such a super-

lattice. However, the reasonable agreement between our calculations and experiment suggests that these effects are not large in the $Ga_{1-x}In_xSb/InAs$ superlattice system.

4. Conclusion

$Ga_{1-x}In_xSb/InAs$ superlattices currently show considerable promise for 8–12 μm detector applications in which high detectivity is required. While manufacturing issues alone may favour these superlattices over $Hg_{1-x}Cd_xTe$, bringing these superlattice detectors to maturity would also ease cooling requirements for background-limited performance. We find that predicted performance benefits over $Hg_{1-x}Cd_xTe$ are magnified at wavelengths beyond 12 μm. Namely, effective masses remain appreciable for near-zero gap superlattices, which should lead to a reduction in tunnelling noise currents, and the substantial splitting between heavy- and light-hole valence bands should suppress the Auger recombination pathway predominant in p-type $Hg_{1-x}Cd_xTe$, with the result that impact ionization noise associated with this channel should be lowered. Of additional practical importance is the relative insensitivity of the calculated effective masses to fluctuations in layer thicknesses.

Lastly, we have explored the dependence of the electronic band structure of these superlattices upon the choice of InSb-like or $Ga_{1-x}In_xAs$-like interfaces. We find that the choice of interfaces shifts the energy gap of a particular superlattice, with the shift increasing in magnitude at longer wavelengths (both in absolute and relative terms). Our calculations show that large (> 1000 cm^{-1}) absorption coefficients can be obtained in structures with InSb-like interfaces.

Acknowledgments

The authors gratefully acknowledge useful discussions with R Baron of Hughes, D A Collins of Caltech, H Ehrenreich of Harvard University and D L Smith of Los Alamos National Laboratories. We are particularly grateful to H Ehrenreich for communicating results prior to publication. We thank J K Neeland for technical assistance. Parts of this work were performed under DARPA/ONR Contracts Nos N00014-89-C-0203 and N00014-89-J-3196.

References

[1] Smith D L and Mailhiot C 1987 *J. Appl. Phys.* **62** 2545
[2] Smith D L and Mailhiot C 1987 *J. Appl. Phys.* **62** 2545
[3] Miles R H, Chow D H and Hamilton W J 1992 *J. Appl. Phys.* **71** 211
[4] Chow D H, Miles R H, J R Söderström and McGill T C 1990 *J. Vac. Sci. Technol.* B **8** 710
[5] Campbell I H, Sela I, Laurich B K, Smith D L, Bolognesi C R, Samoska L A, Gossard A C and Kroemer H 1991 *Appl. Phys. Lett.* **59** 846
[6] Fan W C, Zborowski J T, Golding T D and Shih H D 1992 *J. Appl. Phys.* **71** 2249
[7] Chow D H unpublished
[8] Miles R H unpublished
[9] See, for example, Miles R H, Chow D H and McGill T C 1990 *SPIE Proc.* **1285** 132
[10] Miles R H, Chow D H, Schulman J N and McGill T C 1990 *Appl. Phys. Lett.* **57** 801
[11] Omaggio J P, Meyer J R, Wagner R J, Hoffman C A, Yang M J, Chow D H and Miles R H 1992 *Appl. Phys. Lett.* **61** 207
[12] Omaggio J P, Meyer J R, Wagner R J, Hoffman C A, Yang M J, Chow D H and Miles R H 1993 *Semicond. Sci. Technol.* **8** at press
[13] Kane E O 1966 *Semiconductors and Semimetals* vol 1, ed R K Willardson and A C Beer (New York: Academic) p 75
[14] Smith D L and Mailhiot C 1986 *Phys. Rev.* B **33** 8345
[15] Lawaetz P 1971 *Phys. Rev.* B **4** 3460
[16] *Landolt-Börnstein New Series* 1987 vol III/22a, ed O Madelung (Berlin: Springer)
[17] Bir G L and Pikus G E 1974 *Symmetry and Strain-Induced Effects in Semiconductors* (Jerusalem: Keter)
[18] Sai-Halasz G A, Chang L L, Walter J M, Chang C A and Esaki L 1978 *Solid State Commun.* **27** 935
[19] Smith D L private communication
[20] Grein C H, Young P M and Ehrenreich H 1992 *Appl. Phys. Lett.* to be published
[21] Tuttle G, Kroemer H and English J H 1990 *J. Appl. Phys.* **67** 3032
[22] Chow D H, Miles R H and Hunter A T 1992 *J. Vac. Sci. Technol.* B **10** 888
[23] Schulman J N 1986 *MRS Symp. Proc.* **56** 279
[24] See, for example, Kane E O 1957 *J. Phys. Chem. Solids* **1** 249
[25] Nelson J S, Kurtz S R, Dawson L R and Lott J A 1990 *Appl. Phys. Lett.* **57** 578